

# Grain growth kinetics for B<sub>2</sub>O<sub>3</sub>-doped ZnO ceramics

BERAT YUKSEL\*, T. OSMAN OZKAN

Istanbul University, Engineering Faculty, Metallurgical and Materials Engineering Department,  
Avcilar, 34320, Istanbul, Turkey

Grain growth kinetics in 0.1 to 2 mol % B<sub>2</sub>O<sub>3</sub>-added ZnO ceramics was studied by using a simplified phenomenological grain growth kinetics equation  $G^n = K_0 \cdot t \cdot \exp(-Q/RT)$  together with the physical properties of sintered samples. The samples, prepared by conventional ceramics processing techniques, were sintered at temperatures between 1050 to 1250 °C for 1, 2, 3, 5 and 10 hours in air. The kinetic grain growth exponent value ( $n$ ) and the activation energy for the grain growth of the 0.1 mol % B<sub>2</sub>O<sub>3</sub>-doped ZnO ceramics were found to be 2.8 and 332 kJ/mol, respectively. By increasing B<sub>2</sub>O<sub>3</sub> content to 1 mol %, the grain growth exponent value ( $n$ ) and the activation energy decreased to 2 and 238 kJ/mol, respectively. The XRD study revealed the presence of a second phase, Zn<sub>3</sub>B<sub>2</sub>O<sub>6</sub> formed when the B<sub>2</sub>O<sub>3</sub> content was  $\geq 1$  mol %. The formation of Zn<sub>3</sub>B<sub>2</sub>O<sub>6</sub> phase gave rise to an increase of the grain growth kinetic exponent and the grain growth activation energy. The kinetic grain growth exponent value ( $n$ ) and the activation energy for the grain growth of the 2 mol % B<sub>2</sub>O<sub>3</sub>-doped ZnO ceramics were found to be 3 and 307 kJ/mol, respectively. This can be attributed to the second particle drag (pinning) mechanism in the liquid phase sintering.

Keywords: boron oxide; grain growth; zinc oxide

© Wroclaw University of Technology.

## 1. Introduction

Zinc oxide is an n-type semiconductor with a band gap of 3.37 eV, crystallizing in wurtzite structure [1]. It is widely used in varistors [2], gas sensors [1], in the form of films [3–6], piezoelectric transducers [7] and transparent electrodes for solar cells [8], due to its unique properties. The n-type electrical conductivity of undoped ZnO results from deviations from stoichiometry in the form of interstitial zinc atoms and/or oxygen vacancies. In the applications of ZnO as an electronic material, the control of these native defects is essential since its electrical properties are largely affected not only by extrinsic dopants, but also by native defects [9]. Therefore, the defect chemistry of ZnO has been investigated in a large number of articles. However, the fundamental knowledge on the native defects is still lacking; the defect species that dominate the electrical properties of undoped ZnO still raises a lot of controversy [9–15].

Further increase in the n-type electrical conductivity of ZnO can be achieved by doping with

a trivalent dopant, such as Al, In, Ga and B. As a result, these dopants, called shallow donors, are easily ionized from the new energy levels close to the conduction band in the material. For this reason, considerable attention has been devoted to investigate the effect of Al, In and Ga additions on the electrical, optical and microstructural properties of ZnO [16–18]. In addition, the electrical properties of polycrystalline ZnO ceramics also depend on its microstructure, therefore, it is important to understand the microstructural development of ZnO ceramics during sintering [2]. There have also been a large number of studies addressing the effects of several metal oxide additions, such as Bi<sub>2</sub>O<sub>3</sub>, MnO, and Sb<sub>2</sub>O<sub>3</sub>, on the sintering behaviour of ZnO varistors [2, 19, 20]. However, there are only a few literature reports concerning the electrical and microstructure properties of B<sub>2</sub>O<sub>3</sub>-doped ZnO ceramics [21–26]. Glot and Mazurik reported that the introduction of B<sub>2</sub>O<sub>3</sub> into ZnO ceramics improves the stability of their I-V characteristics [25]. More recently, it has been stated that the electrical stability of ZnO varistors under dc conditions can be improved with the addition of B<sub>2</sub>O<sub>3</sub> using the nano-coating method, which was evidenced by

\*E-mail: berat@istanbul.edu.tr

a smaller degradation rate coefficient and a weaker reduction in resistance of grain boundaries during degradation [26]. However, the exact mechanism of the B<sub>2</sub>O<sub>3</sub> effect on microstructure and electrical properties of ZnO has not been concluded yet. Hence, the aim of the present work is to investigate the effect of B<sub>2</sub>O<sub>3</sub> addition on the densification and microstructure properties of ZnO ceramics in a systematic way. The activation energy analysis of the grain growth in a B<sub>2</sub>O<sub>3</sub>-ZnO system has not been attempted yet. Therefore, a further aim of this work is to study the grain growth kinetics in B<sub>2</sub>O<sub>3</sub>-doped ZnO ceramics which can be determined by using the simplified phenomenological kinetics equation 1:

$$G^n = K_0 \cdot t \cdot \exp(-Q/RT) \quad (1)$$

where G is the average grain size at the time t, n is the kinetic grain growth exponent value, K<sub>0</sub> is a constant, Q is the activation energy for the grain growth, R is the gas constant, and T is the absolute temperature of sintering [2, 19]. According to equation 1, the n value can be determined from the slope of the log (G) versus log (t) linear plot, which is 1/n under isothermal conditions. When equation 1 is expressed in the form:

$$\log(G^n/t) = \log K_0 - 0.434(Q/RT) \quad (2)$$

the activation energy (Q) for the grain growth process can be calculated from the gradient of the Arrhenius plot of log(G<sup>n</sup>/t) versus 1/T [2, 19].

## 2. Experimental

ZnO (99.5 % purity, Metal Bilesikleri A.S., Gebze, Kocaeli, Turkey) and H<sub>3</sub>BO<sub>3</sub> (99.9 % purity) as a source of B<sub>2</sub>O<sub>3</sub> were used to prepare the compositions by the conventional ceramics processing techniques. The powders of ZnO and H<sub>3</sub>BO<sub>3</sub> were weighed according to the molar ratios of the compositions given in Table 1.

The calculated amounts of H<sub>3</sub>BO<sub>3</sub> to yield B<sub>2</sub>O<sub>3</sub> were dissolved in distilled water and then the mixtures of ZnO and H<sub>3</sub>BO<sub>3</sub> were prepared by mechanical mixing in distilled water for 1 h. The mixtures were initially dried at 80 °C and then at

110 °C by stirring frequently in order to mix the H<sub>3</sub>BO<sub>3</sub> homogeneously. After drying, the resulting powders were granulated and uniaxially pressed into discs of 17 mm in diameter and 4 mm in thickness under a pressure of 100 MPa. The samples were sintered at 1050, 1100, 1150, 1200 and 1250 °C for 1, 2, 3, 5 and 10 hours employing a 300 °C/h heating rate in air, then cooled naturally in the furnace. The bulk density of the sintered samples was calculated from their weights and dimensions. The phases were identified by X-ray diffraction (XRD-6000 Shimadzu-Japan) using CuKα radiation at 40 kV/30mA. The microstructure of the samples was studied by a scanning electron microscope (SEM, Jeol JSM 5600) and an optical microscope. Grain size measurements were carried out on the optical micrographs of polished and etched samples using the relation  $G = 1.56 \cdot L$ , where G is the average grain size, L is the average grain-boundary intercept length of a series of random lines on the two micrographs of samples [2, 19].

Table 1. Molar ratios of prepared compositions.

Composition code	ZnO (mol %)	B <sub>2</sub> O <sub>3</sub> (mol %)
Z	100	–
B01	99.9	0.1
B05	99.5	0.5
B1	99	1
B15	98.5	1.5
B2	98	2

## 3. Results and discussion

The X-ray diffraction (XRD) measurements were carried out in order to determine crystal phases formed in the samples of selected compositions. The XRD results demonstrated that the undoped ZnO as well as 0.1 and 0.5 mol % B<sub>2</sub>O<sub>3</sub>-doped samples revealed only the ZnO phase (ASTM No.: 36-1451). Fig. 1 illustrates the XRD patterns of 1 and 2 mol % B<sub>2</sub>O<sub>3</sub>-doped ZnO samples. As can be seen in the Fig. 1, the XRD study revealed the presence of a second phase related to the

$B_2O_3$  as  $Zn_3B_2O_6$  (ASTM No.: 37-1486) formed at 1 and 2 mol %  $B_2O_3$  content.

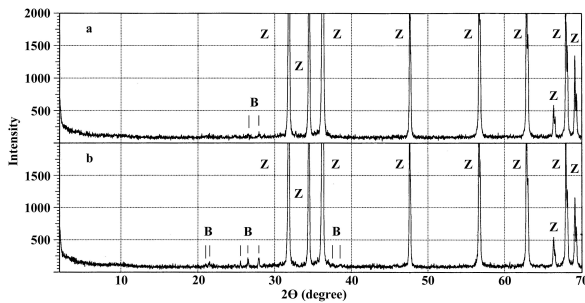


Fig. 1. XRD analysis of (a) B1 and (b) B2 samples sintered at 1050 °C for 1 hour (Z; ZnO, B;  $Zn_3B_2O_6$ ).

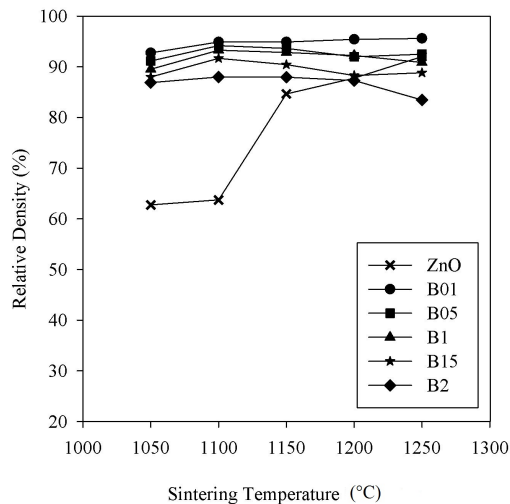
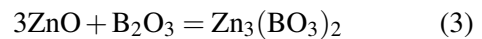


Fig. 2. Relative density of Z, B01, B05, B1, B15 and B2 samples as a function of sintering temperature for 1 hour.

Fig. 2 shows the relative density of undoped and 0.1 to 2 mol %  $B_2O_3$ -doped ZnO samples as a function of sintering temperature for 1 hour sintering process. The relative densities of the undoped ZnO samples sintered at 1050 °C and 1100 °C for 1 hour were 63 and 64 % of the theoretical density of ZnO, respectively. It can be seen in this figure that the density of undoped ZnO samples increased with increasing the sintering temperature. The density value of 92 % was obtained when the undoped ZnO samples were sintered at 1250 °C for 1 hour.

The 0.1 and 0.5 mol %  $B_2O_3$ -doped samples had a relative density ranging from 91 to 96 % of the theoretical density. It is clear that the addition of  $B_2O_3$  had a marked effect on the densification of ZnO ceramics particularly at  $T \leq 1150$  °C. On the other hand, the density of  $B_2O_3$ -doped samples was slightly decreased above 1 mol %  $B_2O_3$  content when the sintering temperature was higher than 1150 °C. The possible reasons might be attributed to the reduced sintering driving force due to the formation of  $Zn_3B_2O_6$  phase above 1 mol %  $B_2O_3$  content and also, the increased amount of porosity among the large grains of ZnO resulting from the rapid grain growth induced by the liquid phase sintering at higher sintering temperatures. The exact mechanism of the  $B_2O_3$  effect remains unknown today; however, it is derived from the low melting point of the  $B_2O_3$  (450 °C) which has a good effect on the grain growth of ZnO [26]. According to Abduev et al., any boron compound, forming a boron oxide during sintering, improves the conditions of sintering providing a liquid phase at the grain boundaries, which results in synthesis of ceramics with a high density [21]. Similarly, Liu et al. reported that the low melting point of  $B_2O_3$  caused the liquid phase sintering and the grain growth of ZnO started at a lower temperature and further accelerated the growth of ZnO grains. They also reported that  $B_2O_3$  reacted with ZnO grain and formed the  $Zn_3(BO_3)_2$  phase through the reaction 3:



The formation of  $Zn_3(BO_3)_2$  at the grain boundaries may inhibit grain growth by pinning movement of the grain boundaries. Therefore, the grain size and density of ZnO increased first then decreased, while the added amount was above 3.5 mol %  $B_2O_3$  [24].

Fig. 3 shows the selected SEM micrographs of the undoped ZnO samples sintered at 1100, 1150, 1200 and 1250 °C for 1 hour. The sintering at 1100 °C for 1 hour resulted in a porous and fine (<1 μm) crystalline microstructure (Fig. 3a). The samples sintered at 1150 °C for 1 hour also revealed a fine-grained microstructure with a grain

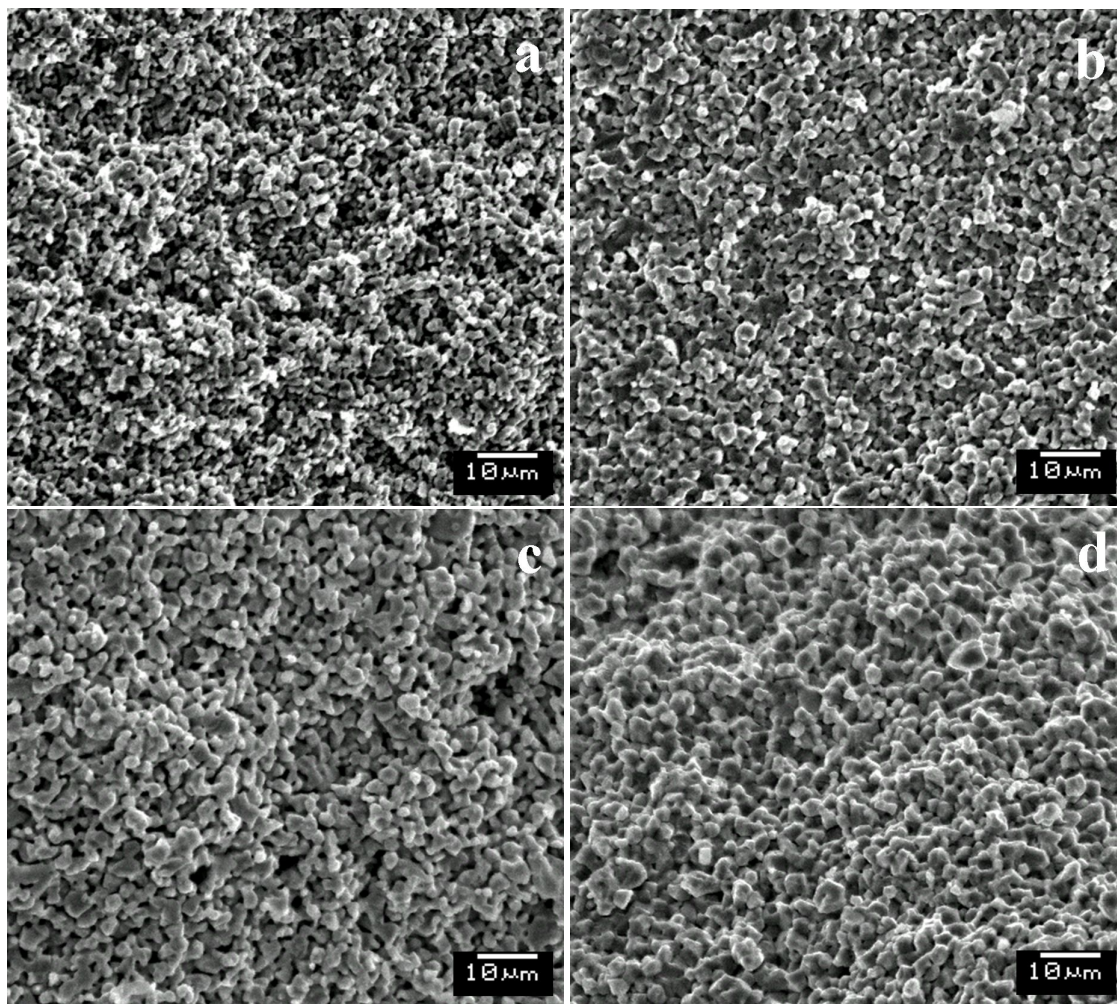


Fig. 3. SEM micrographs of Z samples sintered at 1100 °C/1 h (a), at 1150 °C/1 h (b), at 1200 °C/1 h (c) and at 1250 °C/1 h (d).

size of around 1  $\mu\text{m}$  (Fig. 3b). When the sintering temperature was increased to 1200 and 1250 °C for 1 hour, the grain size of samples increased to about 5  $\mu\text{m}$  (Fig. 3c, 3d). Fig. 4 shows the optical micrographs of the 0.1 mol %  $B_2O_3$ -added samples sintered at 1050, 1150 and 1250 °C for 1 and 5 hours. The average grain size of samples sintered at 1050 °C for 1 and 5 hours is 6  $\mu\text{m}$  and 11  $\mu\text{m}$ , respectively. Even a small amount of  $B_2O_3$  addition resulted in the grain growth of zinc oxide at lower sintering temperature for shorter sintering time and the samples exhibited a uniform microstructure. It can also be observed in Fig. 4 that the grain size of 0.1 mol %  $B_2O_3$ -added samples increased with the increasing sintering temperature

and sintering time. Fig. 5 shows the SEM micrographs of 0.1 to 2 mol %  $B_2O_3$ -doped ZnO samples sintered at 1100 °C for 1 hour. As can be seen in Fig. 5, the  $B_2O_3$  additions resulted in a dense microstructure with quite uniform grains of around 10  $\mu\text{m}$  in size compared with undoped ZnO samples shown in Fig. 3. Similar microstructures were observed for the  $B_2O_3$ -doped ZnO samples at other sintering temperatures in this study.

Fig. 6 shows the average grain size of the 0.1 to 2 mol %  $B_2O_3$ -doped ZnO samples as a function of sintering temperature for various sintering times. Similar plots could not be constructed for the undoped ZnO samples in this study. As mentioned above, the undoped ZnO samples had a fine

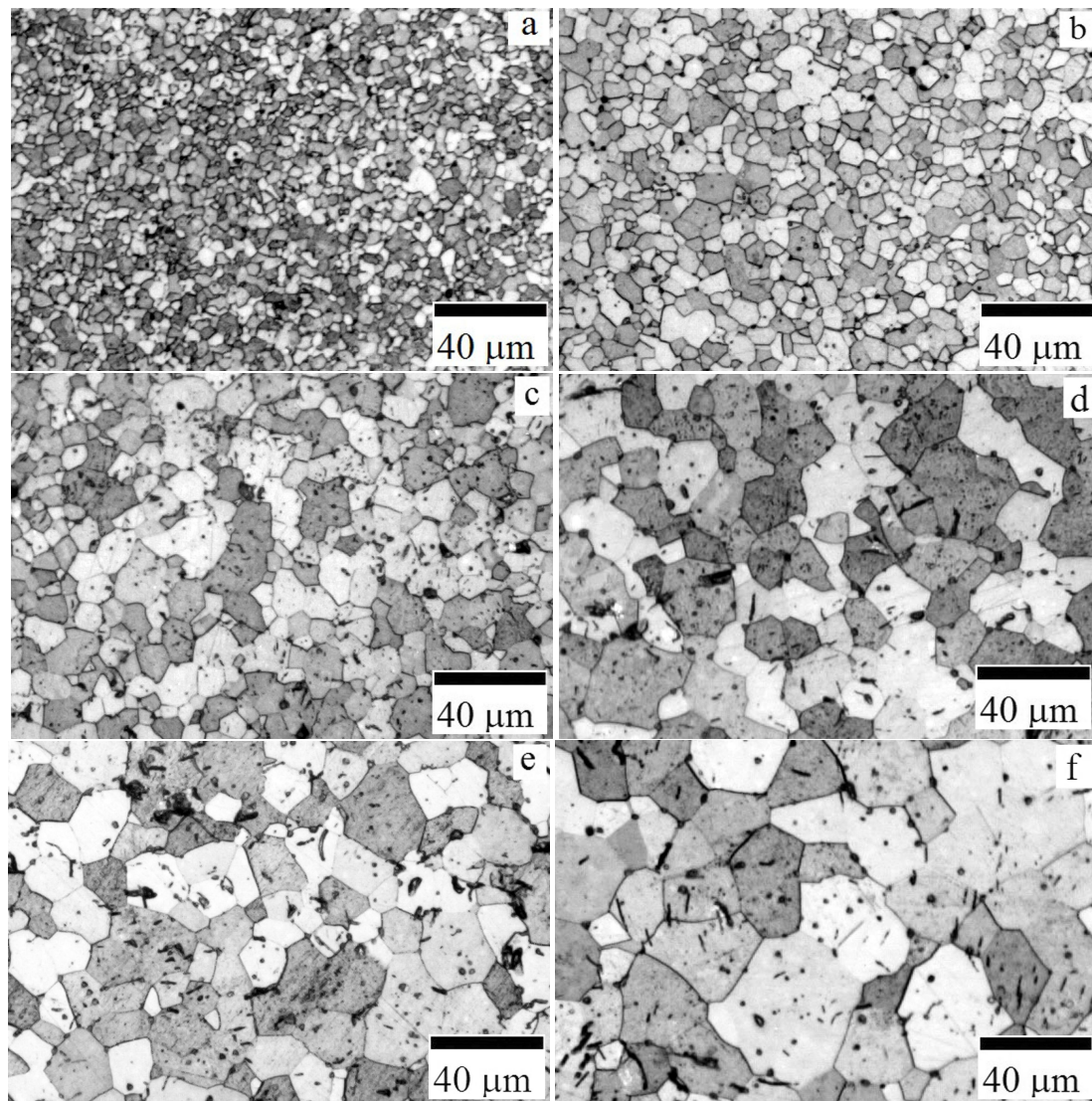


Fig. 4. Optical micrographs of 0.1 mol %  $B_2O_3$ -added samples sintered at 1050 °C (a) for 1 h, (b) for 5 h, 1150 °C (c) for 1 h, (d) for 5 h and 1250 °C (e) for 1 h, (f) for 5 h.

grain size, less than 5  $\mu\text{m}$ , which gave rise to a large amount of grain pull-outs, while polishing samples for the optical observation and the grain growth in the undoped zinc oxide samples occurred at high sintering temperature for prolonged sintering time. In general, the grain size of  $B_2O_3$ -doped ZnO samples increases with increasing sintering temperature for prolonged sintering time; on the other hand, the density and grain size of the investigated samples increased first and then decreased with the increasing  $B_2O_3$  content above 0.5 mol %. The highest average grain size of 80

and 59  $\mu\text{m}$  were correspondingly obtained for the 0.5 mol % and 2 mol %  $B_2O_3$ -doped samples sintered at 1250 °C for 10 hours, respectively.

Fig. 7 depicts the  $\log G$  (grain size) versus  $\log t$  (time) plots for the 0.1 to 2 mol %  $B_2O_3$ -doped samples sintered at 1150 °C. There have been many studies concerning the grain growth of pure ZnO. Although the grain growth exponent value ( $n$ ) of 3 was consistently observed in these studies, the activation energies for the grain growth process of pure ZnO have been reported in the range of 224 to 461 kJ/mol [2, 27–29].

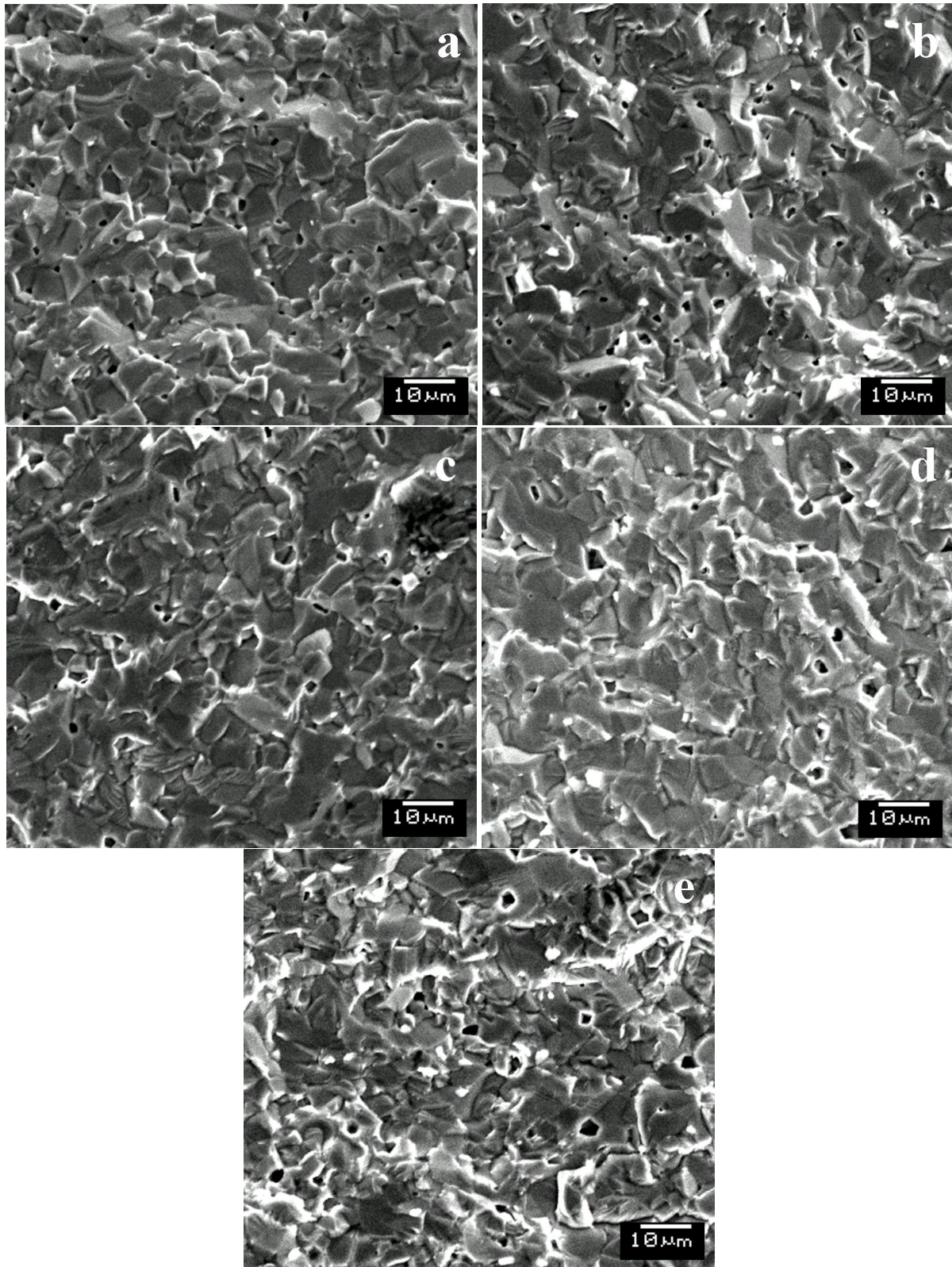


Fig. 5. SEM micrographs of B01 (a), B05 (b), B1 (c), B15 (d) and B2 (e) samples sintered at 1100 °C for 1 hour.

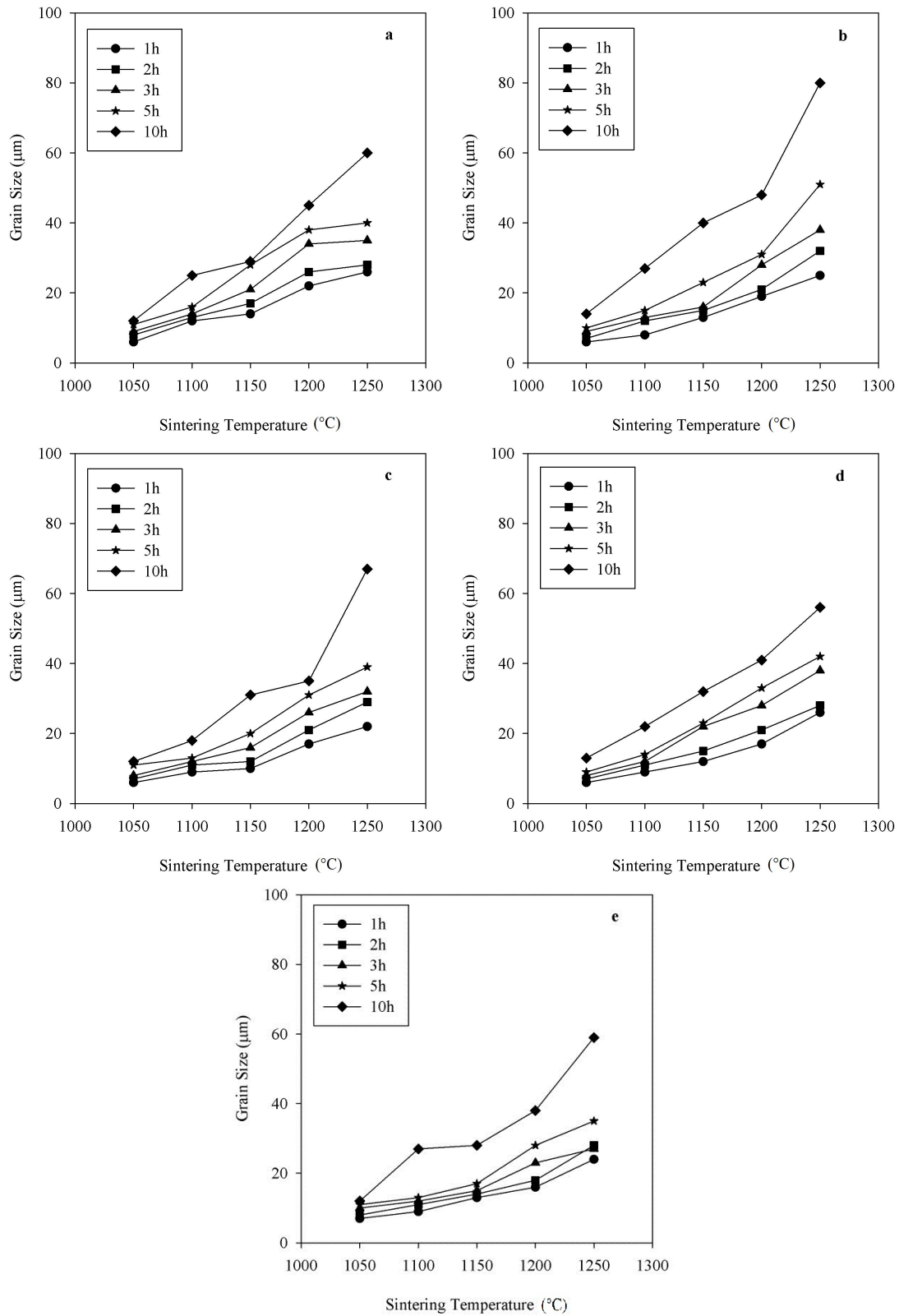


Fig. 6. Average grain sizes of B01 (a), B05 (b), B1 (c), B15 (d) and B2 (e) samples as a function of sintering temperature for various sintering times.

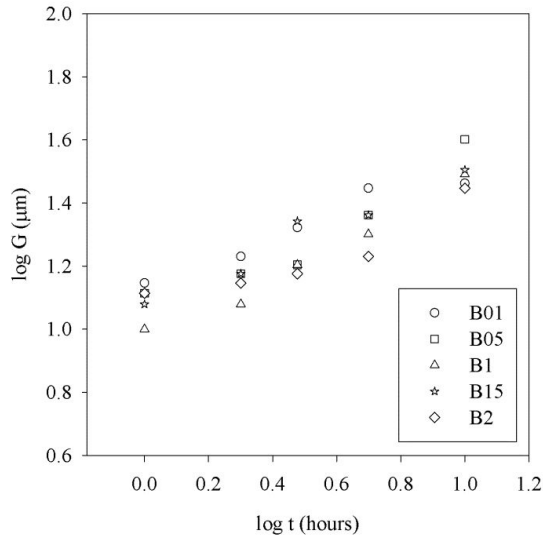


Fig. 7. Log G (grain size) versus log t (time) plots for the 0.1 to 2 mol % B<sub>2</sub>O<sub>3</sub>-doped samples sintered at 1150 °C.

Table 2. Calculated kinetic grain growth exponent (n) and activation energy (Q).

Composition code	n values at 1150 °C	Q (kJ/mol)
B01	2.8	332
B05	2	255
B1	2	238
B15	2.3	285
B2	3	307

Senda and Bradt calculated the activation energy as  $224 \pm 16$  kJ/mol for sintering a pure ZnO system [2]. On the other hand, Norris and Parravano measured the early stages of neck growth of ZnO spheres from 1050 to 1250 °C and found much larger activation energy of 440 to 461 kJ/mol as well as smaller grain sizes [28]. This difference can probably be attributed to the processing conditions and to the raw material properties, such as powder particle morphology, particle size distribution or impurities contained within the powder, creating grain-boundary drag, decreasing grain-boundary mobility, thus, the grain size, by slowing the rate of the grain growth [2]. Fig. 8 shows the Arrhenius plot of  $\log(G^3/t)$  versus  $(1/T)$  constructed for the 0.1 to 2 mol % B<sub>2</sub>O<sub>3</sub>-doped samples. The activation energy of the grain growth can be obtained from the

slopes of the Arrhenius plots. Table 2 illustrates the calculated average kinetic grain growth exponent (n) values and the activation energies (Q) for the 0.1 to 2 mol % B<sub>2</sub>O<sub>3</sub> doped ZnO samples.

In comparison with the grain size of the undoped ZnO samples, obtained in this study (Fig. 3a – d) and also reported in the literature [27, 30, 31], the addition of B<sub>2</sub>O<sub>3</sub> significantly promoted the grain growth of ZnO and resulted in the uniform microstructure due to the low melting temperature of B<sub>2</sub>O<sub>3</sub> [32]. As mentioned previously, the grain growth exponent value (n) of 3 was consistently observed for pure ZnO [2, 27–29]. According to Hng and Halim, the small value of n obtained for ZnO – 1 mol %V<sub>2</sub>O<sub>5</sub> system indicated that the grain growth was much faster than for pure ZnO [33]. The spinel-particle drag effect on the grain growth of ZnO was investigated in the solid-state sintering system of ZnO–Al<sub>2</sub>O<sub>3</sub> and this effect gave rise to an increase in the grain growth exponent and the grain growth activation energy of ZnO due to the formation of ZnAl<sub>2</sub>O<sub>4</sub> [34]. In addition, Bradt et al. reported that a second particle drag (pinning) mechanism controlling the grain growth can be effective both in the liquid-phase sintering and in the solid phase sintering [35]. These results are in agreement with our results. The smaller n value obtained for B01, B05 and B1 compositions than that of undoped ZnO, reported in the literature, showed that a small amount of B<sub>2</sub>O<sub>3</sub> addition ( $\leq 1$  mol %) was beneficial to obtain faster grain growth in ZnO. When the amount of B<sub>2</sub>O<sub>3</sub> addition was above 1 mol %, the formation of Zn<sub>3</sub>B<sub>2</sub>O<sub>6</sub> phase gave rise to an increase of the grain growth kinetic exponent and the grain growth activation energy compared to 1 mol % B<sub>2</sub>O<sub>3</sub>-added ZnO ceramics. This can be attributed to the second particle drag (pinning) mechanism in the liquid phase sintering.

## 4. Conclusion

The effect of B<sub>2</sub>O<sub>3</sub> additions at the levels of 0.1 to 2 mol % on the grain growth of ZnO was investigated. The B<sub>2</sub>O<sub>3</sub> additions increased the densification of ZnO particularly in the initial stage

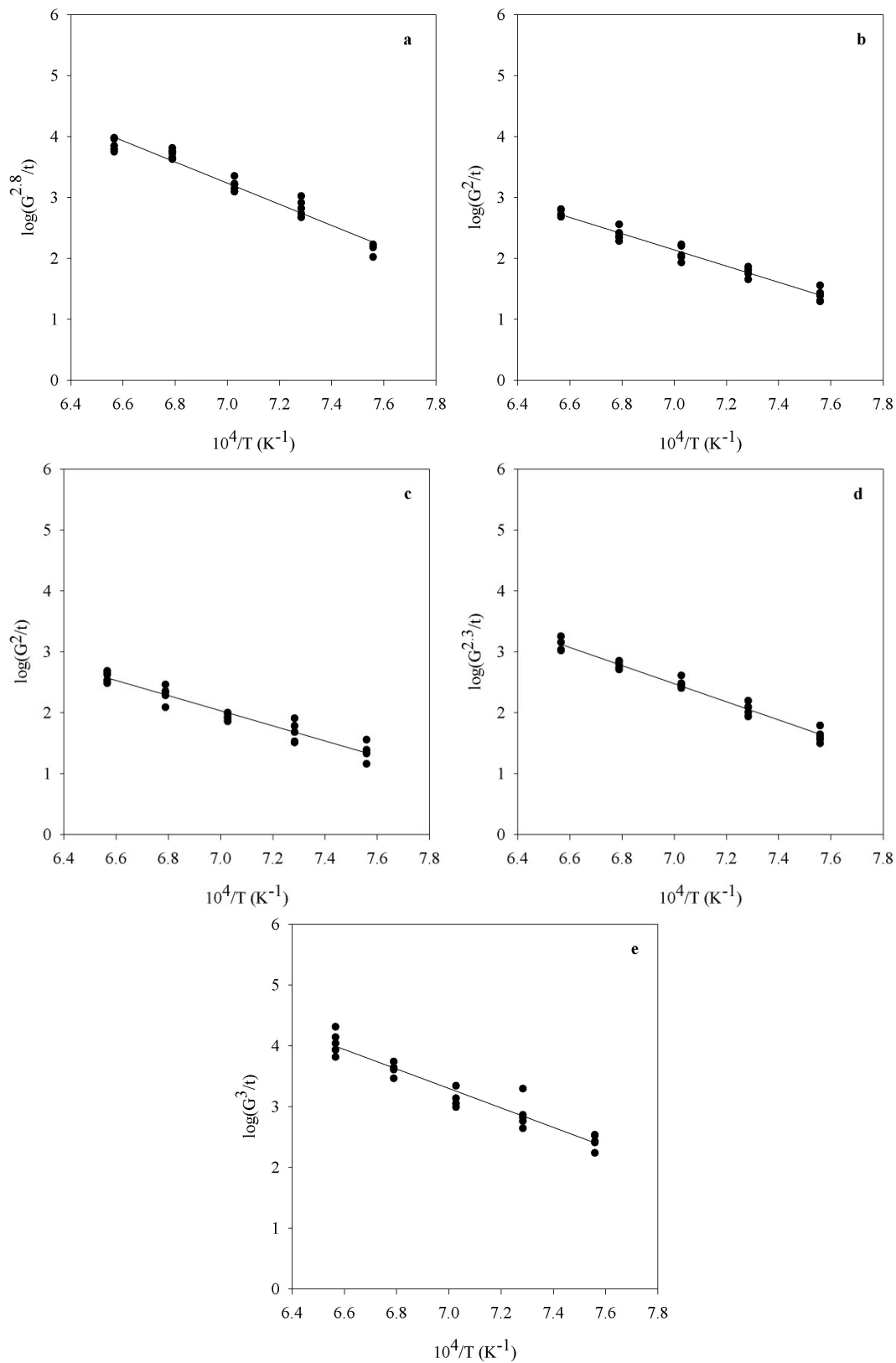


Fig. 8. Arrhenius plots of  $\log(G^n/t)$  versus  $(1/T)$  constructed for B01 (a), B05 (b), B1 (c), B15 (d) and B2 (e) samples.

of sintering. The addition of B<sub>2</sub>O<sub>3</sub> up to 1 mol % resulted in a decrease in the average kinetic grain growth exponent (n) values and an increase in the activation energy for the grain growth. The smaller “n” values compared to that of pure ZnO given in the literature indicate the faster grain growth rate for B<sub>2</sub>O<sub>3</sub>-doped ZnO ceramics. When the amount of B<sub>2</sub>O<sub>3</sub> addition was above 1 mol %, the formation of Zn<sub>3</sub>B<sub>2</sub>O<sub>6</sub> phase gave rise to an increase of the grain growth kinetic exponent and the activation energy of the grain growth. In conclusion, addition of small amount of B<sub>2</sub>O<sub>3</sub> as a sintering aid up to 1 mol % was beneficial for lowering the sintering temperature and improving the grain growth of ZnO.

### Acknowledgements

This work was supported by the Scientific Research Projects Coordination Unit of Istanbul University. Project number T-699 and UDP-16345. It was partially based on a PhD. thesis pursued by Berat Yuksel.

### References

- [1] SUCHEA M., CHRISTOULAKIS S., MOSCHOVIS K., KATSARAKIS N., KIRIAKIDIS G., *Thin Solid Films*, 515 (2006), 551.
- [2] SENDA T., BRADT R.C., *J. Am. Ceram. Soc.*, 73 (1990), 106.
- [3] LOKHANDE B.J., PATIL P.S., UPLANE M.D., *Physica B*, 302 – 303 (2001), 59.
- [4] CHEN X.L., XU B.H., XUE J.M., ZHAO Y., WEI C.C., SUN J., WANG Y., ZHANG X.D., GENG X.H., *Thin Solid Films*, 515 (2007), 3753.
- [5] ISHIZAKI H., IMAIZUMI M., MATSUDA S., IZAKI M., ITO T., *Thin Solid Films*, 411 (2002), 65.
- [6] TAHAR R.B.H., TAHAR N.B.H., *J. Mater. Sci.*, 40 (2005), 5285.
- [7] GAO P.X., WANG Z.L., *J. Appl. Phys.*, 97 (2005), 044304 1.
- [8] ISLAM M.N., SAMANTARAY B.K., CHOPRA K.L., ACHARYA H.N., *Sol. Energ. Mat. Sol. C*, 29 (1993), 27.
- [9] OBA F., NISHITANI S. R., ISOTANI S., ADACHI H., TANAKA I., *J. Appl. Phys.*, 90 (2001), 824.
- [10] HAGEMARK K. I., *J. Solid State Chem.*, 16 (1976), 293.
- [11] MAHAN G.D., *J. Appl. Phys.*, 54 (1983), 3825.
- [12] ZIEGLER E., HEINRICH A., OPPERMAN H., STRÖVER G., *Phys. Status Solidi A*, 66 (1981), 635.
- [13] NEUMANN G., *Phys. Status Solidi B*, 105 (1981), 605.
- [14] MARKEVICH I. V., KUSHNIRENKO V. I., BORKOVSKA L. V., BULAKH B. M., *Phys. Status Solidi C*, 3 (4) (2006), 942.
- [15] HAUSMANN A., SCHALLENBERGER B., *Z. Phys. B*, 31 (1978), 269.
- [16] HAN J., MANTAS P.Q., SENOS A.M.R., *J. Eur. Ceram. Soc.*, 21 (2001), 1883.
- [17] YOON M.H., LEE S.H., PARK H.L., KIM H.K., JANG M.S., *J. Mater. Sci. Lett.*, 21 (2002), 1703.
- [18] ZHANG Y., HAN J., *Mater. Lett.*, 60 (2006), 2522.
- [19] TOPLAN O., GUNAY V., OZKAN T.O., *Ceram. Int.*, 23 (1997), 251.
- [20] HAN J., MANTAS P.Q., SENOS A.M.R., *J. Eur. Ceram. Soc.*, 20 (2000), 2753.
- [21] ABDUEV A.K., ASVAROV S., AKHMEDOV A.K., KAMILOV I.K., *US Patent* 20090218735 A1, 3. Sep. 2009.
- [22] KUSHNIRENKO V.I., MARKEVICH I.V., RUSAVSKY A.V., *Radiat. Meas.*, 45 (2010), 468.
- [23] LEVINSON L. M., *US patent* 4460623, 17. Jul. 1984.
- [24] LIU F., XU G., DUAN L., LI Y., LI Y., CUI P., *J. Alloy. Compd.*, 509 (2011), L56.
- [25] GLOT A. B., MAZURIK S. V., *Inorg. Mater.*, 36 (2000), 636.
- [26] CHENG L., LI G., YUAN K., MENG L., ZHENG L., *J. Am. Ceram. Soc.*, 95 (2012), 1004.
- [27] GUPTA T. K., COBLE R. L., *J. Am. Ceram. Soc.*, 51 (1968), 521.
- [28] NORRIS L.F., PARRAVANO G., *J. Am. Ceram. Soc.*, 46 (1963), 449.
- [29] NICHOLSON G.C., *J. Am. Ceram. Soc.*, 48 (1965), 214.
- [30] WONG J., *J. Appl. Phys.*, 51 (1980), 4453.
- [31] ASOKAN T., IYENGAR G.N., NAGABHUSHANA G.R., *J. Mater. Sci.*, 22 (1987), 2229.
- [32] FAN J., SALE F.R., *J. Am. Ceram. Soc.*, 20 (2000), 2743.
- [33] HNG H. H., HALIM L., *Mater. Lett.*, 57 (2003), 1411.
- [34] HAN J., MANTAS P.Q., SENOS A.M.R., *J. Mater. Res.*, 16 (2001), 459.
- [35] BRADT R.C., NUNES S.I., SENDA T., SUZUKI H., BURKETT S.L., *Grain Growth*, in: GERMAN R.M., MESSING G.L., CORNWALL R.G. (Eds.), *Sintering Technology*, Marcel Dekker, New York, 1996, p. 389.

Received 2014-05-13

Accepted 2014-12-08